

NOTICE

**CERTAIN DATA
CONTAINED IN THIS
DOCUMENT MAY BE
DIFFICULT TO READ
IN MICROFICHE
PRODUCTS.**

Conf-4010185-18

BNL-NUREG-44993

MELCOR Simulation of Long-Term Station Blackout
at Peach Bottom

I. K. Madni

BNL-NUREG--44993

Safety Integration Group
Safety & Risk Evaluation Division
Department of Nuclear Energy
Brookhaven National Laboratory
Upton, NY 11973

DE91 006348

ABSTRACT

This paper presents the results from MELCOR (Version 1.8BC) calculations of the Long-Term Station Blackout Accident Sequence, with failure to depressurize the reactor vessel, at the Peach Bottom (BWR Mark I) plant, and presents comparisons with Source Term Code Package (STCP) calculations of the same sequence. This sequence assumes that batteries are available for six hours following loss of all power to the plant. Following battery failure, the reactor coolant system (RCS) inventory is boiled off through the relief valves by continued decay heat generation. This leads to core uncover, heatup, clad oxidation, core degradation, relocation, and, eventually, vessel failure at high pressure. STCP has calculated the transient out to 13.5 hours after core uncover. MELCOR calculations have been carried out to 16.7 hours after core uncover. The results include the timing of key events, pressure and temperature response in the reactor vessel and containment, hydrogen production, and the release of source terms to the environment.

INTRODUCTION

MELCOR is a fully integrated computer code that models all phases of the progression of severe accidents in nuclear power plants [1]. It is being developed for the U.S. Nuclear Regulatory Commission by Sandia National Laboratories (SNL) and is designed to provide an improved severe accident/source term analysis capability relative to the older Source Term Code Package (STCP) [2]. BNL has a program with the NRC to verify and apply the MELCOR code to severe accident analysis for several plants.

This paper presents the results from a MELCOR calculation of a Long-Term Station Blackout Accident Sequence with failure to depressurize the reactor vessel. Peach Bottom, a boiling water reactor with Mark I containment, was used in the analysis. The paper also compares MELCOR predictions with STCP

* This work was performed under the auspices of the U.S. Nuclear Regulatory Commission under Contract DE-AC02-76CH00016.

MASTER

DISTRIBUTION OF THIS DOCUMENT IS UNLIMITED

f

calculations for the same sequence [3]. This sequence assumes that batteries are available for six hours following loss of all power to the plant. Station blackout sequences have often been determined to be important contributors to the risk from severe accidents [4]. Following battery failure, the reactor coolant system (RCS) inventory is boiled off through the relief valves by continued decay heat generation. This leads to core uncover, heatup, clad oxidation, core degradation, relocation, and, eventually, vessel failure at high pressure. STCP has calculated the transient out to 13.5 hours after core uncover. MELCOR calculations have been carried out to 16.7 hours after core uncover. The results include the timing of key events, pressure and temperature response in the reactor vessel and containment, hydrogen production, and the release of source terms to the environment.

The main contribution of this paper is in reporting a successful MELCOR plant simulation of a severe accident sequence resulting in source terms to the environment. MELCOR is a relatively new code, and every new application brings it into uncharted territory where new code errors are uncovered. This application was no exception, and after several code errors were uncovered and resolved, the calculations eventually went to completion. These applications thus allow MELCOR to gain maturity as a source-term analysis tool. The comparisons with the older, more widely used STCP, while being a byproduct of this effort, do serve as a useful yardstick and lend credibility to the results from the new code.

MELCOR PLANT MODEL

Figure 1 is a schematic of the Mark I containment design for the Peach Bottom plant [5].

Nodalization

The MELCOR Peach Bottom model is a modified version of the untested input deck that was received from Sandia National Laboratory in 1988. It consists of 19 control volumes (6 for the RCS, 3 for the primary containment, 9 for the secondary containment, including refueling bay, and 1 for the environment); 33 flow paths (16 in the RCS and primary containment and 17 in the secondary containment); and 66 heat structures (20 in the RCS and containment and the rest in the secondary containment). The reactor core is modeled with 33 core cells (i.e., 3 concentric radial rings and 11 axial levels). Levels 7 through 11 comprise the active core region, and levels 1 through 6 are the lower plenum including the core plate which is Level 6. Figures 2 [6] and 3 show the MELCOR nodalization for the Peach Bottom plant and its reactor core, respectively.

Some Features of Simulation

MELCOR either explicitly or parametrically models all key in-vessel and ex-vessel phenomena. In-vessel phenomena modeled include the thermal-hydraulic behavior of the reactor coolant system (RCS), fuel rod heatup, zircaloy oxidation, and hydrogen generation, core degradation, and lower head response. Fission product release, transport, deposition, and revaporization are also treated. Ex-vessel phenomena include core/concrete interactions, primary and

secondary containment thermal-hydraulic and heat structure response, hydrogen burning and detonation, aerosol behavior, and the impact of engineered safety features (e.g., pools) on thermal-hydraulics and radionuclide transport.

Each cell may contain one or more types of components, including intact fuel, cladding, canister walls (for BWRs), other structures, such as control rods or guide tubes, and particulate debris, which may each contain several materials (e.g., UO_2 , Zircaloy, ZrO_2). Oxidation and heat transfer by radiation, conduction, and convection are calculated separately for each component. A simple candling model treats the downward flow and refreezing of molten core materials, thereby forming layers of conglomerate debris on lower cell components which may lead to flow blockages and molten pools. Failure of core structures, such as the core plate as well as lower head heatup and failure followed by debris ejection, are treated by simple parametric models. For this simulation, the failure was triggered by a user-specified temperature corresponding to zero yield strength. Upon vessel failure, steam and gases are discharged through the opening. The default option allows solid debris and molten material to be discharged at a rate calculated from the pressure difference, flow area, and a loss coefficient.

Models for a broad spectrum of radionuclide behavior are included in MELCOR. By default, MELCOR uses the 15 classes recommended in the MELCOR Phenomena Assessment [7]. These default classes include two nonradioactive classes for bulk material aerosols (H_2O and concrete) and are summarized in Table 1. The user may also create new classes to model the stoichiometric combination of elements in existing classes, such as Cs and I.

The release of fission products from fuel is modeled in MELCOR using either CORSOR or CORSOR-M [8]. Depending on user choice, these rate equations are then modified for the appropriate surface area to volume ratio of the fuel/debris as compared to the ratios represented in the experiments on which the models are based. If the clad is intact as determined by the gap release model discussed below, any released material is added to the gap inventory. This model is also used for the release of nonradioactive material. Release of radionuclide from the fuel-clad gap is modeled simplistically by a user-specified clad failure temperature (1173K for all calculations in this report). When the clad temperature in any cell in a given ring exceeds this clad failure temperature, or if the clad in a cell in this ring melts completely away, the entire gap inventory for that ring is instantaneously released. The elemental and compound forms of each class are both considered in the release model. For the Cs class, the elemental form is Cs but the compound form may be CsOH. The difference in the elemental and compound molecular weights determines the amount of nonradioactive material that is added to the released mass. In the Cs class example, the mass of OH is added to the total mass of the Cs class.

Release during core-concrete reactions is treated by the VANESA [9] models. Aerosol dynamics involving agglomeration and deposition are calculated with the MAEROS [10] equations, while condensation and evaporation from aerosol and heat structure surfaces are calculated using the TRAP-MELT [11] models.

DISCLAIMER

This report was prepared as an account of work sponsored by an agency of the United States Government. Neither the United States Government nor any agency thereof, nor any of their employees, makes any warranty, express or implied, or assumes any legal liability or responsibility for the accuracy, completeness, or usefulness of any information, apparatus, product, or process disclosed, or represents that its use would not infringe privately owned rights. Reference herein to any specific commercial product, process, or service by trade name, trademark, manufacturer, or otherwise does not necessarily constitute or imply its endorsement, recommendation, or favoring by the United States Government or any agency thereof. The views and opinions of authors expressed herein do not necessarily state or reflect those of the United States Government or any agency thereof.

RESULTS AND COMPARISONS WITH STCP

In the base case, MELCOR simulation of the station blackout scenario presented here, the maximum allowable timestep size (Δt_{max}) is specified as 10 seconds, and the fuel release model selected is CORSOR with surface-to-volume ratio correction. The containment is assumed to fail in the drywell at a pressure of 9.1 bars (~132 psia), which is consistent with the STCP assumption [1], and with analysis of the steel shell performed by Ames Laboratory [12]. Computing time required for 60,000 seconds of problem time was 34,200 seconds (WARP=1.75) on a VAX 6340 computer.

Key Events

Table 2 summarizes the predicted timing of key events for the MELCOR and STCP [1] calculations, starting with core uncover when the water level has dropped to the top of the active fuel. MELCOR predicts clad melting and relocation to start at about 99 minutes, with fuel melting following about 18 minutes later. STCP, on the other hand, does not distinguish between the different core components and calculates core melt to start at 114 minutes. MELCOR models the core in 3 radial rings and predicts partial core collapse to occur in the innermost ring at 154 minutes, while STCP calculates gross core collapse at 166.8 minutes. This can explain why the predicted dryout of the lower plenum occurs so much quicker for STCP. Vessel failure occurs in MELCOR at 274 minutes when the penetrations in ring 1 fails, whereas STCP calculates gross lower head failure at 205 minutes. This difference can be explained because core relocation occurs more gradually in MELCOR, via "candling" and debris formation. Note that following vessel breach, steam, non-condensable gases, and aerosols escape from the opening, while ejection of debris to the cavity occurs much later. This MELCOR-predicted time lag will greatly diminish the perceived probability of occurrence of DCH following this high pressure core melt sequence. MELCOR predicts drywell failure to occur at 7.1 hours, or 40 minutes later than the STCP calculation. This is again related to the earlier vessel failure predicted by STCP. Both codes predict deflagrations to occur in the reactor building and refueling bay, shortly after drywell failure.

In-Vessel Behavior

The response of important in-vessel parameters as calculated by MELCOR are shown in Figures 4 through 10. Figure 4 shows the pressure response of the separator (CV350) and dryer (CV360) regions. The total pressure remains approximately constant due to the pressure-relieving operation of the SRV valves. However, the sharp downward pressure spike in steam partial pressures corresponds to a sharp positive pressure spike in the partial pressure of hydrogen which is produced from zircaloy oxidation. The sharp drop in total pressure starting at ~16,500 seconds corresponds to vessel failure and subsequent depressurization of the vessel. Figure 5 shows the swollen liquid level in the core (CV340), bypass (CV330), annulus (CV310), and lower plenum (CV320), as a function of time. The rapid level drop in the lower plenum is seen to start at the same time that partial core collapse occurs in ring 1 (~9,250 seconds), leading to eventual lower head dryout at 12,378 seconds. Figures 6 and 7 show the cumulative flow of steam and hydrogen, respectively, through the SRV lines. The curves taper off

and become flat for $t > 16,500$ seconds, indicating that flow through these lines stops following vessel failure and depressurization.

Figures 8 and 9 show masses of fuel in various axial levels of the core in the innermost ring. The sharp drop in mass at one level and a corresponding sharp mass increase at a lower level indicates downward relocation. MELCOR calculates the maximum temperature in the core to be 2500 K, occurring in cell 111 ~7,000 seconds after core uncover. STCP predicts peak core temperature of 4100°F (~2530 K), occurring ~6,850 seconds after core uncover.

Figure 10 shows the MELCOR-predicted cumulative in-vessel hydrogen production, which reaches in excess of 1300 kg by the end of the calculation, 60,000 seconds after core uncover.

Ex-Vessel Behavior

The primary containment pressure and temperature histories calculated by MELCOR are presented in Figures 11 through 17. In Figures 11 and 16, it can be seen that failure of the reactor vessel leads to rapid pressurization of both the drywell and wetwell, but the pressure stays below the nominal failure level. Containment failure is calculated to occur at about 426 minutes after core uncover due to the combination of an elevated suppression pool temperature (Figure 17) and the buildup of non-condensable gas. The curves from STCP calculations show similar trends. Failure of the primary containment is followed shortly by several hydrogen burns in the reactor building and refueling bay. Their timings relative to containment failure are similar for both MELCOR and STCP. The predicted duration of deflagration is longer for MELCOR than for STCP. This is because the MELCOR plant model considers many compartments in the reactor building, with delays in burn propagation from one compartment to the next, while STCP models the entire reactor building as one volume.

Figure 18 shows the temperature history of metallic and oxidic debris layers in the cavity and Figure 19 shows the cumulative masses of non-condensable gases released from core-concrete interactions.

Fission Product Transport and Release to Environment

The overall behavior of fission products and decay heat calculated by MELCOR is shown in Figures 20 through 23. Figure 20 shows the cumulative release of radioactive fission product mass from the fuel, along with deposited and released mass of aerosol and vapor components. Total released radioactive mass in-vessel is about 800 kg. Figures 21 and 22 show the in-vessel and ex-vessel releases, respectively, of CsOH, Te, and CsI. Note that in CsOH, only Cs is the radioactive component. It can be seen from the figures that the Cs and I releases occur predominantly in-vessel, whereas more of the Te release occurs ex-vessel. Figure 23 shows the location history of decay heat, both in- and ex-vessel. It can be seen that, with successive penetration failures in the three rings, the core decay heat drops in steps, as cavity decay heat increases in steps, while total decay heat decreases gradually with time.

Prior to vessel failure, fission products are transported to the suppression pool via the SRV lines, and thereafter, they enter the drywell directly. Following containment failure, fission products leak from the drywell into the reactor building, where they travel through the various compartments, and the refueling bay. Table 3 shows the fractional distribution of fission products in various regions of the plant and the environment at the end of the calculation from both MELCOR and STCP. Note that the Cs fractions for MELCOR in the table were obtained by weighted addition of Cs fractions in CsI form (Class 16) and in CsOH form (Class 2), as follows:

$$f(\text{Cs}) = 0.92f(\text{Class 2}) + 0.08f(\text{Class 16}) \quad (1)$$

The coefficients, 0.92 and 0.08, in Eq. (1), were obtained from the distribution of Cs between the two classes. MELCOR-calculated I mass in the form of free iodine (Class 4) was seen to be several orders of magnitude smaller than I mass in the form of CsI (Class 16). Hence, MELCOR-calculated I fractions in Table 3 were assumed equal to the fractions of CsI.

A comparison of environmental releases between MELCOR and STCP reveals significant differences. MELCOR predicts much lower environmental release fractions of Sr, La, Ce, and Ba, and STCP predicts lower fractions of I, Cs, and Ru. MELCOR and STCP predict similar release and retention of I and Cs from the fuel during in-vessel core meltdown; however, the higher environmental release fractions of I and Cs from MELCOR can be attributed to late revaporization from the RCS after the core debris penetrates the reactor vessel. This phenomenon is not modeled in STCP, and, therefore, the revaporization model in MELCOR represents an important advance in modeling capability. Note that since Te is mostly associated with ex-vessel release due to core/concrete interactions, the revaporization of Te from the RCS has no impact on its total release to the environment. The lower refractory releases is because MELCOR calculates debris ejection into the cavity over a much longer period of time, based on successive penetration failures in the three rings, while STCP assumes the release of all of the core at the time of vessel breach. The MELCOR meltdown model, therefore, results in less vigorous core concrete interactions than STCP, leading to lower release of the fission products associated with this phase of the accident. These two models represent credible variations on possible core meltdown configurations and should be taken into account as part of an uncertainty study.

ACKNOWLEDGEMENTS

The author wishes to extend his appreciation to several individuals who have been very helpful throughout this project. In particular, he wishes to acknowledge the help and cooperation of the Development Staff at SNL for providing the untested input deck which served as the starting point of this investigation, for useful discussions, and for resolving code errors in a timely manner as they were uncovered at various stages of the calculation; W. T. Pratt and E. G. Cazzoli of BNL for many helpful discussions and for reviewing the manuscript; B. Agrawal, R. Foulds, C. Tinkler, and F. Eltawila of the U. S. Nuclear Regulatory Commission for their continued support and guidance throughout this project. A special note of thanks is due to Jean Frejka for her excellent preparation of this manuscript.

REFERENCES

1. R. S. Denning, et al., "Radionuclide Release Calculations for Selected Severe Accident Scenarios-BWR, Mark I Design," NUREG/CR-4624, BMI-2139, Vol. 1, July 1986.
2. R. M. Summers, et al., "MELCOR 1.8.0: A Computer Code for Severe Nuclear Reactor Accident Source Term and Risk Assessment Analyses," NUREG/CR-5531, SAND90-0364, to be published.
3. J. A. Gieseke, et al., "Source Term Code Package: A User's Guide," NUREG/CR-4587, BMI-2138, April 1986.
4. Reactor Risk Reference Report, Draft for Comment, NUREG-1150, Vol. 1, February 1987.
5. M. Silberberg, et al., "Reassessment of the Technical Bases for Estimating Source Terms," NUREG-0956, July 1986.
6. S. Dingman, Private Communication, December 1988.
7. R. M. Summers, et al., "MELCOR In-Vessel Modeling," Proceedings of the Fifteenth Water Reactor Safety Information Meeting, NUREG/CP-0090, p. 384, October 1987.
8. M. R. Kuhlman, et al., "CORSOR User's Manual," NUREG/CR-4173, BMI-2122, March 1985.
9. D. A. Powers, et al., "VANESA, A Mechanistic Model of Radionuclide Release and Aerosol Generation During Core Debris Interactions with Concrete," NUREG/CR-4308, SAND85-1370, 1986.
10. F. Gelbard, "MAEROS User Manual," NUREG/CR-1391, SAND80-0822, 1982.
11. H. Jordan and M. R. Kuhlman, "TRAP-MELT2 User's Manual," NUREG/CR-4205, BMI-2124, 1985.
12. L. G. Greimann, et al., "Reliability Analysis of Steel Containment Strength," Iowa State University, NUREG/CR-2442, June 1982.

Table 1
Material Classes in MELCOR [2]

Class Name	Representative	Member Elements
1. Noble Gases	Xe	He, Ne, Ar, Kr, Xe, Rn, H, N
2. Alkali Metals	Cs	Li, Na, K, Rb, Cs, Fr, Cu
3. Alkaline Earths	Ba	Be, Mg, Ca, Sr, Ba, Ra, Es, Fm
4. Halogens	I	F, Cl, Br, I, At
5. Chalcogens	Te	O, S, Se, Te, Po
6. Platinoids	Ru	Ru, Rh, Pb, Re, Os, Ir, Pt, Au, Ni
7. Early Transition Elements	Mo	V, Cr, Fe, Co, Mn, Nb, Mo, Tc, Ta, W
8. Tetravalents	Ce	Ti, Zr, Hf, Ce, Th, Pa, Np, Pu, C
9. Trivalents	La	Al, Sc, Y, La, Ac, Pr, Nd, Pm, Sm, Eu, Gd, Tb, Dy, Ho, Er, Tm, Yb, Lu, Am, Cm, Bk, Cf
10. Uranium	U	U
11. More Volatile Main Group	Cd	Cd, Hg, Zn, As, Sb, Pb, Tl, Bi
12. Less Volatile Main Group	Sn	Ga, Ge, In, Sn, Ag
13. Boron	B	B, Si, P
14. Water	H ₂ O	H ₂ O
15. Concrete	---	---

Table 2
MELCOR and STCP-Predicted Timing of Key Events

Key Event	Time (min)	
	MELCOR	STCP
Core uncovery	0.0	0.0
Start zircaloy oxidation	76.0	
First gap release of fission products	76.8	
Start melt and relocation	117.0	114.0
Core collapse	154.4 (partial) ring 1	166.8
Lower plenum dryout	206.3	176.3
Vessel failure	274.0	205.0
Reactor vessel depressurized	275.1	
Start debris ejection to cavity	341.2	205.1
Drywell failure	426.0	386.0
Start deflagrations in reactor building	426.4	386.5
End deflagrations in reactor building	427.6	386.9
Start deflagrations in refueling bay	429.4	390.6
End deflagrations in refueling bay	430.8	390.7

Table 3
Fractional Distribution of Fission Products by Group in Plant and Environment

Species	RCS		Wetwell		Drywell		Cavity		Reactor Building		Refueling Bay		Environment	
	MELCOR	STCP	MELCOR	STCP	MELCOR	STCP	MELCOR	STCP	MELCOR	STCP	MELCOR	STCP	MELCOR	STCP
I	0.404	0.67	0.146	0.23	0.325	7.8E-02	0.0	0.0	3.43E-02	4.2E-03	5.64E-03	5.8E-05	8.56E-02	7.8E-03
Cs	0.334	0.74	0.14	0.14	0.307	8.8E-02	0.0	0.0	4.36E-02	4.9E-03	9.49E-03	6.2E-04	0.164	9.0E-03
Te	2.6E-02	0.35	1.13E-02	3.6E-02	0.107	7.3E-02	0.797	0.23	3.01E-02	0.19	1.01E-02	1.1E-02	1.78E-02	0.10
Sr	5.29E-02	9.7E-04	9.88E-03	2.9E-02	8.48E-02	0.31	0.76	0.16	4.0E-02	0.26	1.12E-02	1.7E-02	4.13E-02	0.21
Ru	5.51E-03	1.3E-06	2.89E-04	3.3E-07	2.67E-04	1.1E-07	0.993	1.0	3.61E-04	5.3E-07	7.19E-05	4.8E-08	8.85E-04	3.2E-07
La	4.3E-03	1.3E-07	1.54E-05	4.1E-03	7.48E-03	1.2E-02	0.984	0.94	2.8E-03	2.4E-02	1.0E-03	1.4E-03	8.23E-04	1.7E-02
Ce	4.27E-03	0.0	6.05E-06	5.3E-03	7.4E-06	1.8E-02	0.996	0.91	7.89E-06	3.8E-02	1.69E-06	2.2E-03	1.88E-05	2.8E-02
Ba	5.29E-02	1.9E-02	9.88E-03	5.2E-02	8.48E-02	0.16	0.76	0.38	4.0E-02	0.22	1.12E-02	1.3E-02	4.13E-02	0.15

MARK I CONTAINMENT (Peach Bottom)

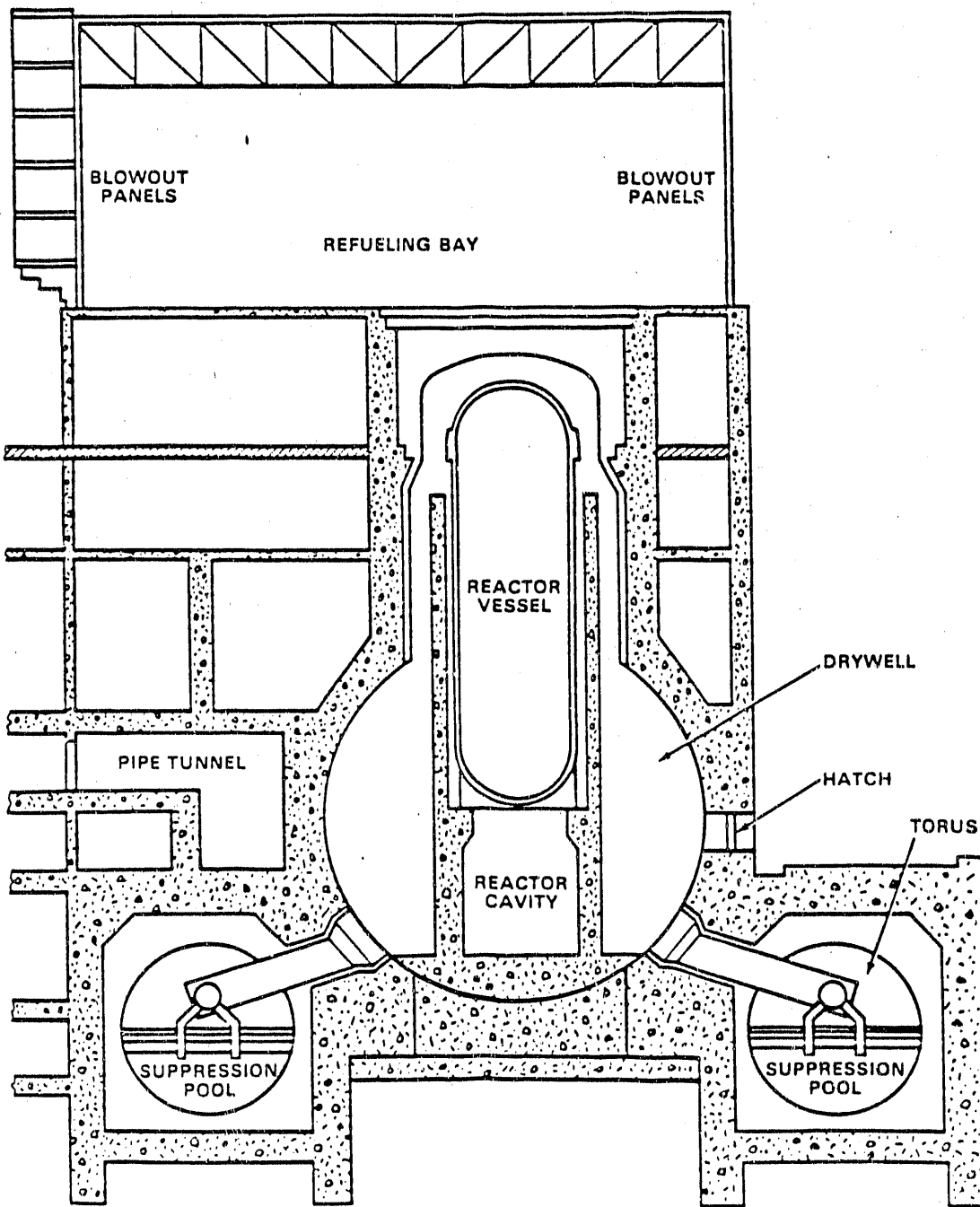


Figure 1 Schematic of the Containment Design for the Peach Bottom Plant [8]

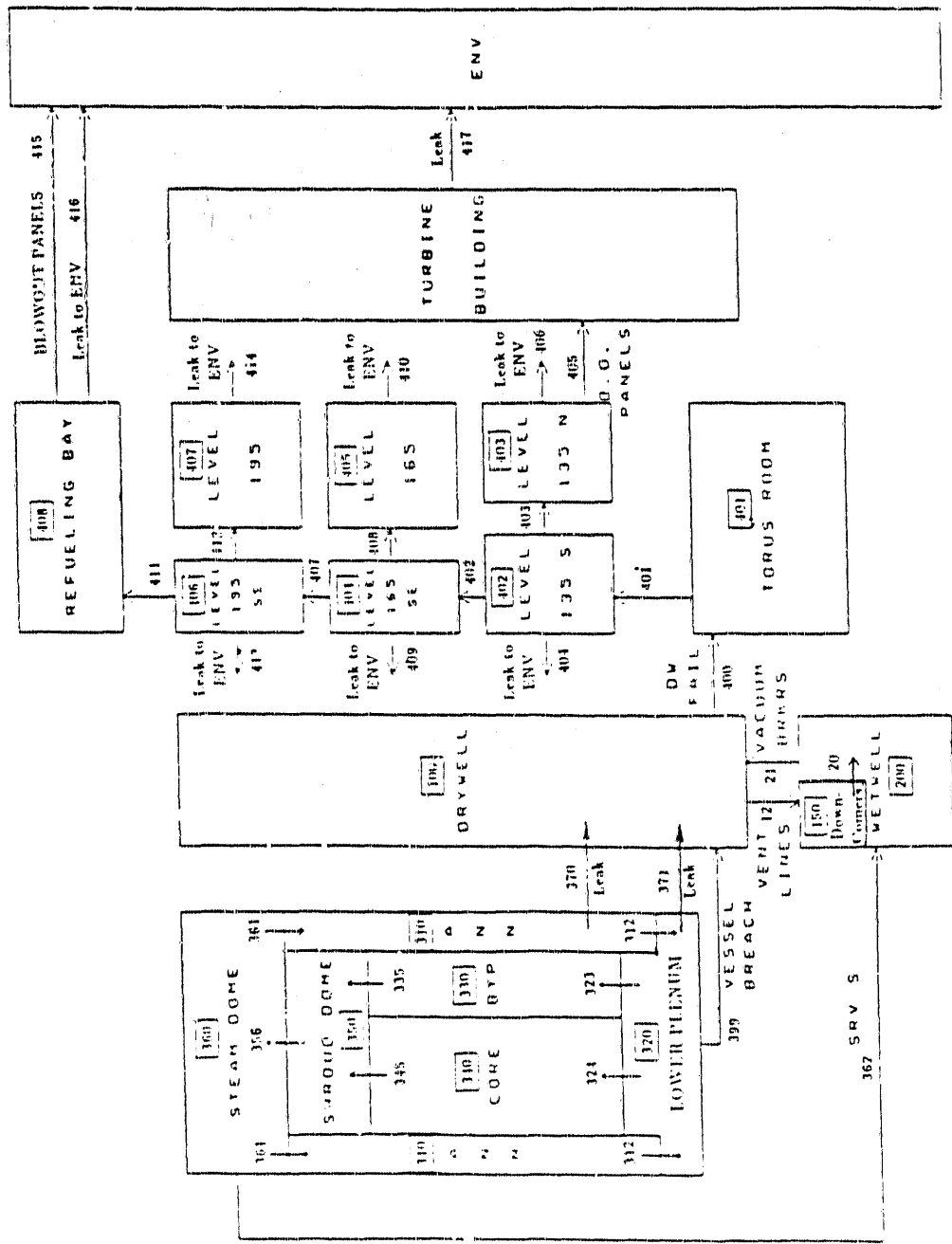


Figure 2 Peach Bottom plant Nodalization for MELCOR [6]

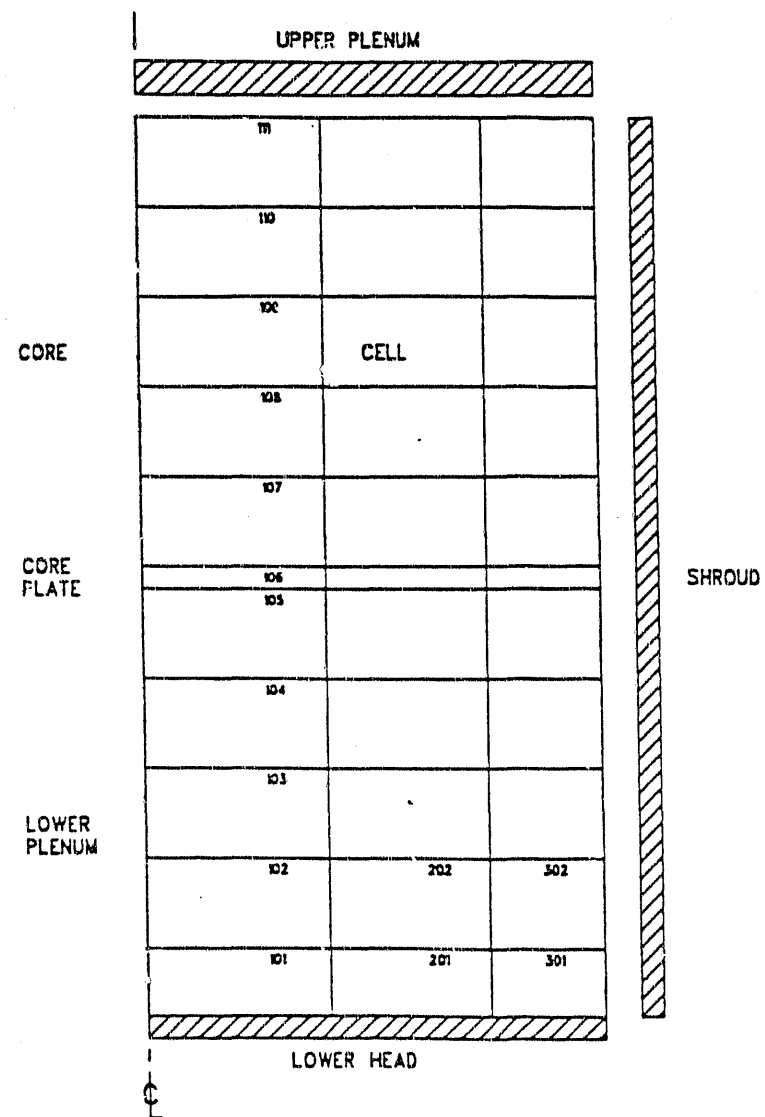


Figure 3 Reactor Core Nodalization

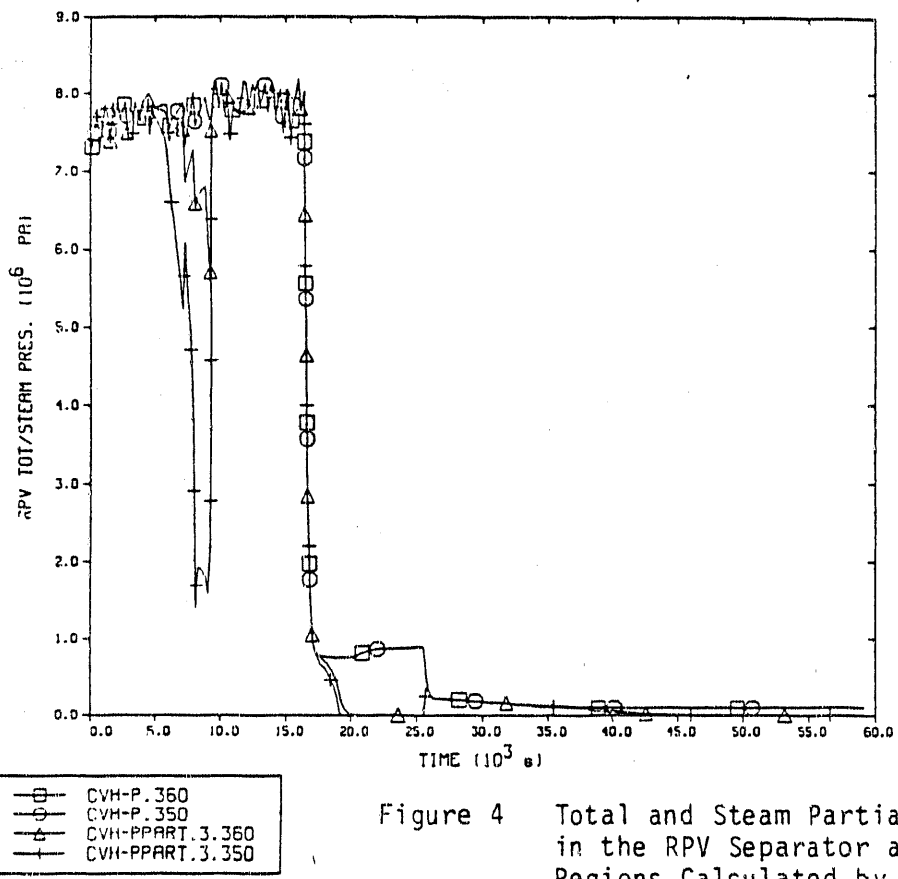


Figure 4 Total and Steam Partial Pressures in the RPV Separator and Dryer Regions Calculated by MELCOR

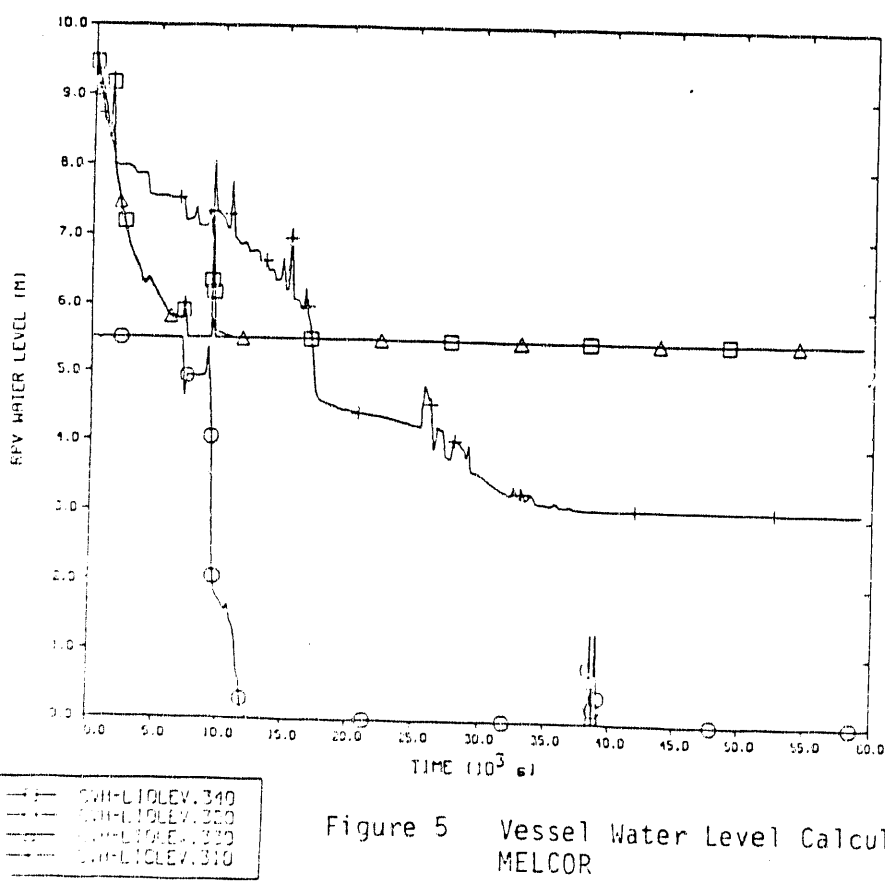


Figure 5 Vessel Water Level Calculated by MELCOR

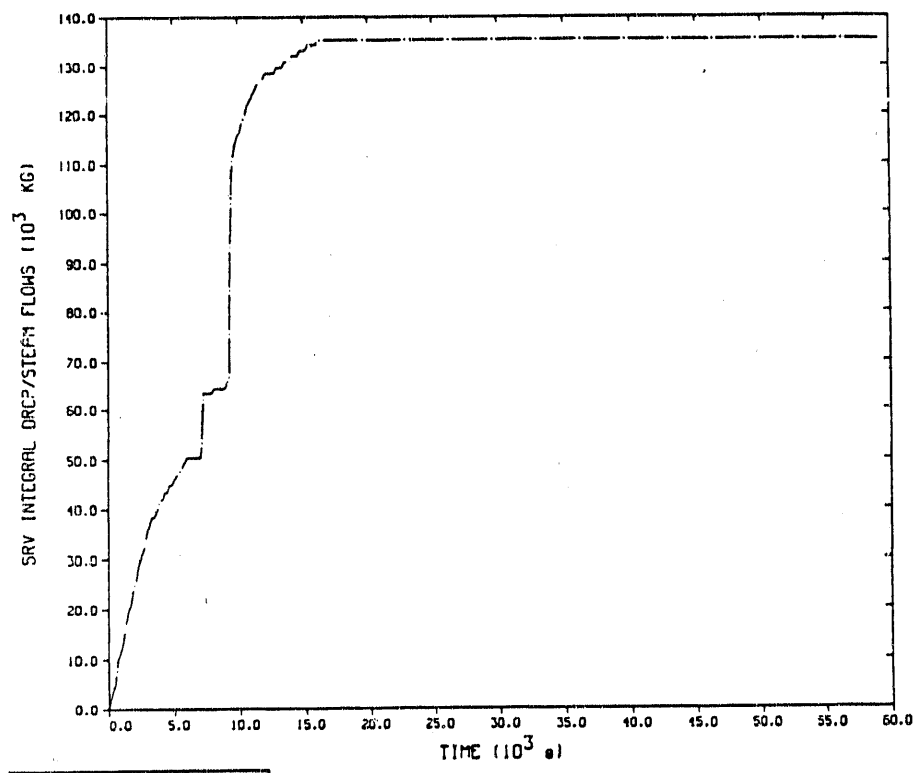


Figure 6 MELCOR-Calculated Cumulative Steam Flow Through the SRV Line

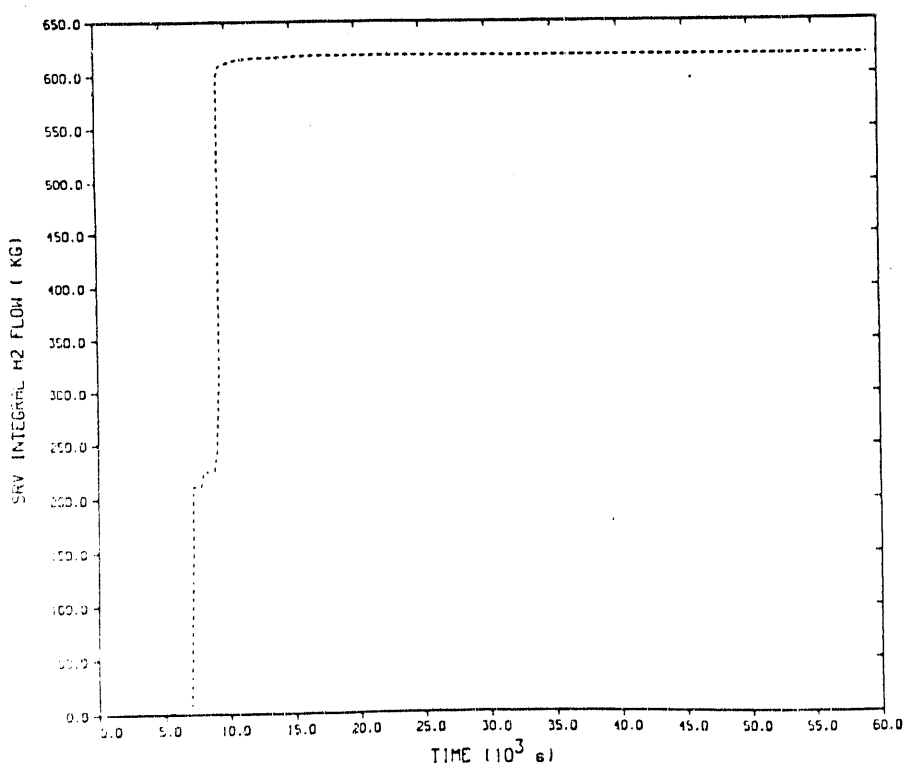
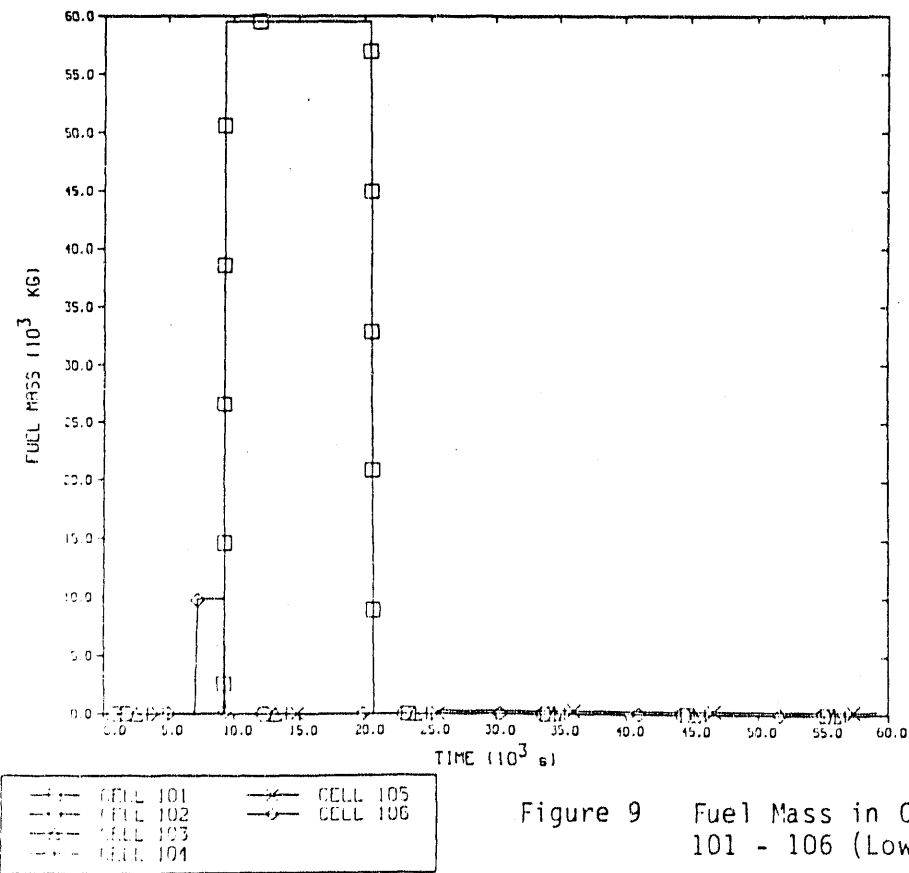
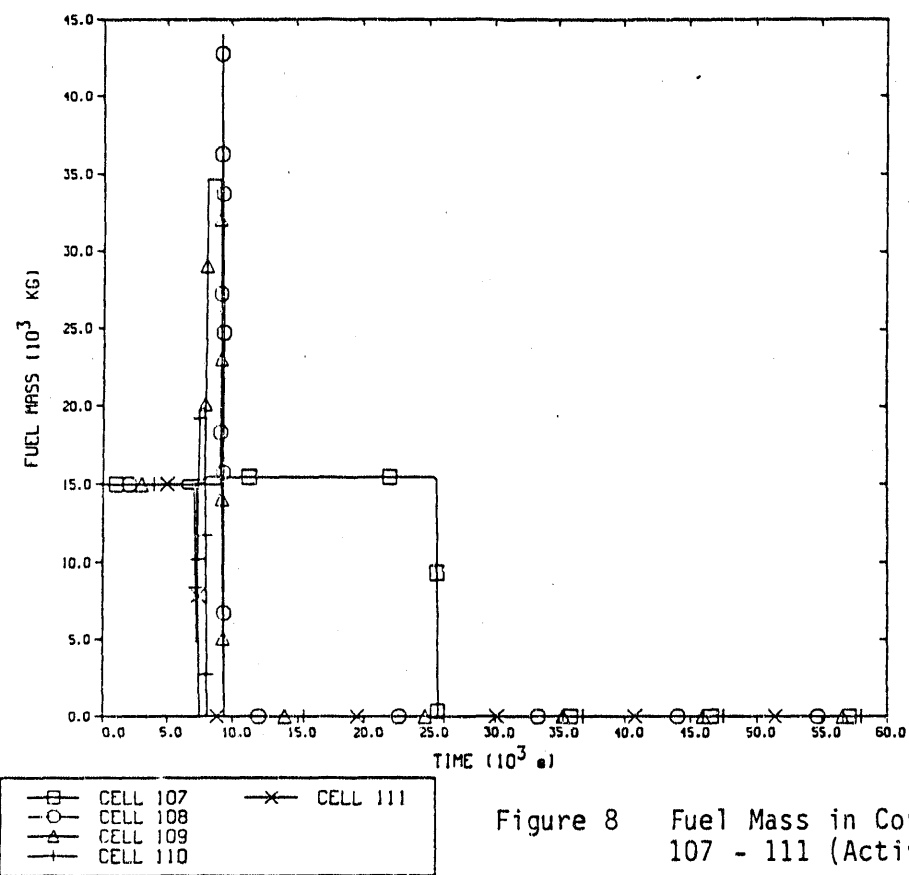


Figure 7 MELCOR-Calculated Cumulative Hydrogen Flow Through the SRV Line



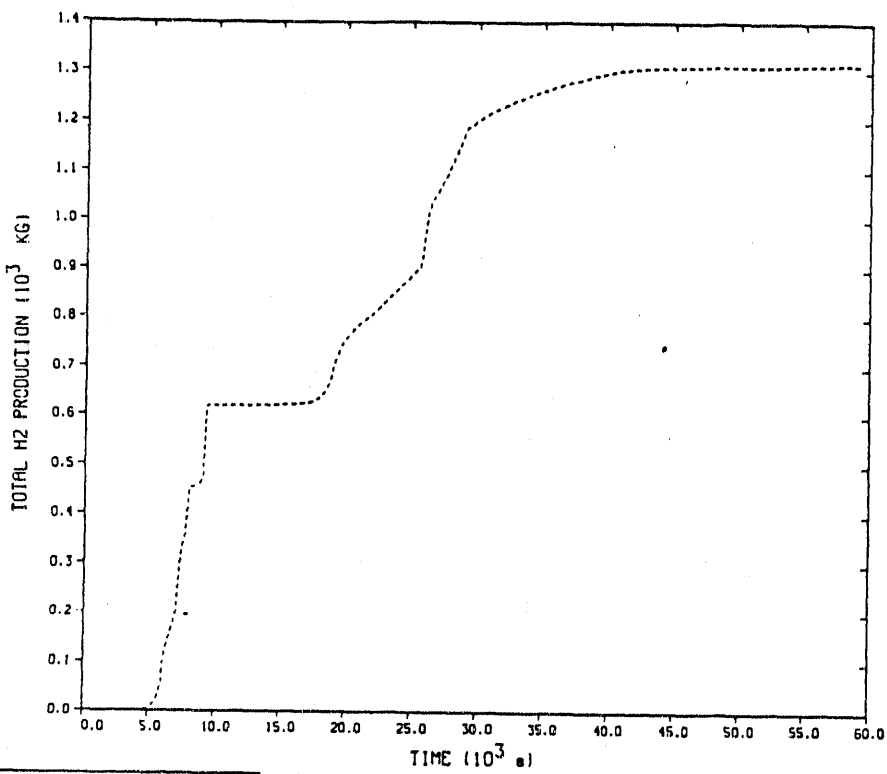


Figure 10 Cumulative Hydrogen Production
Calculated by MELCOR

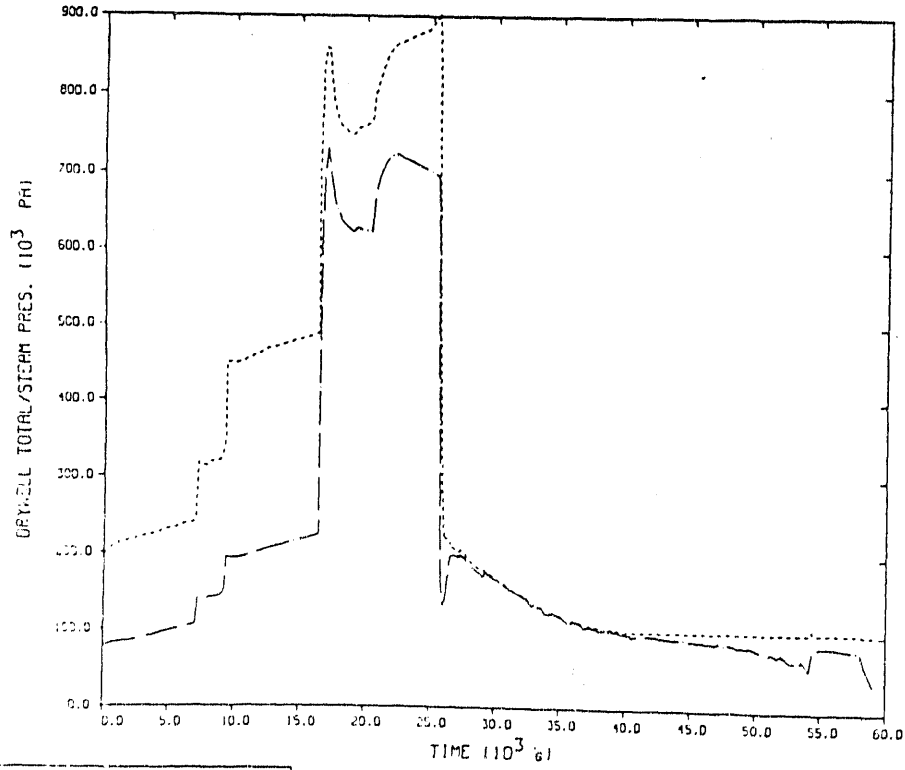


Figure 11 Total and Steam Partial Pressure
History in the Drywell

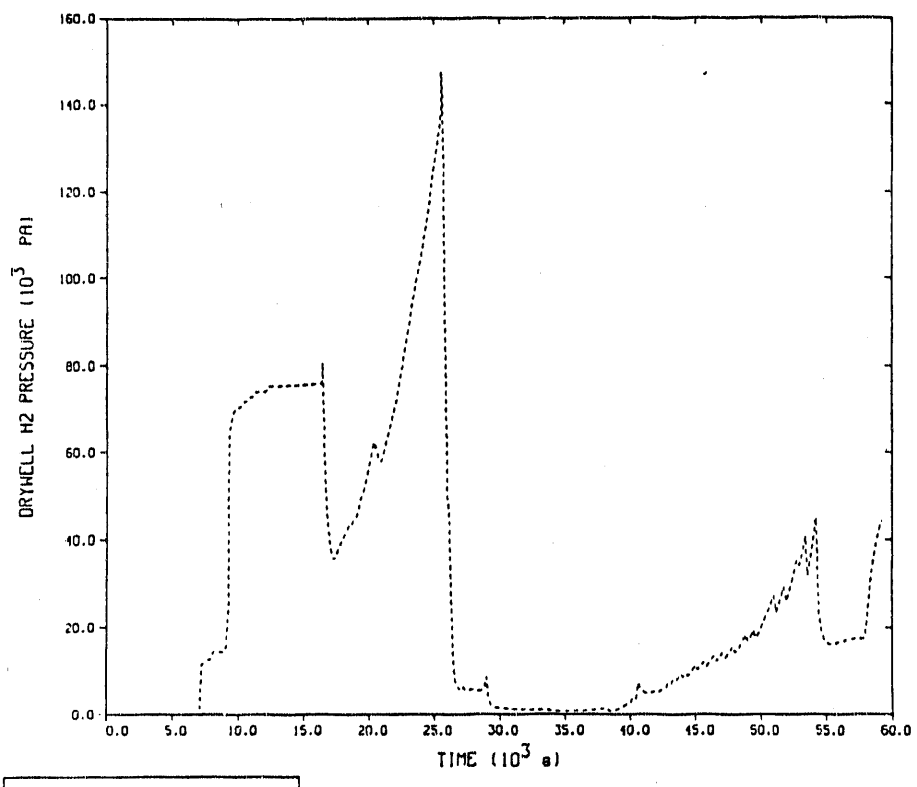


Figure 12 Pressure History of Hydrogen in the Drywell

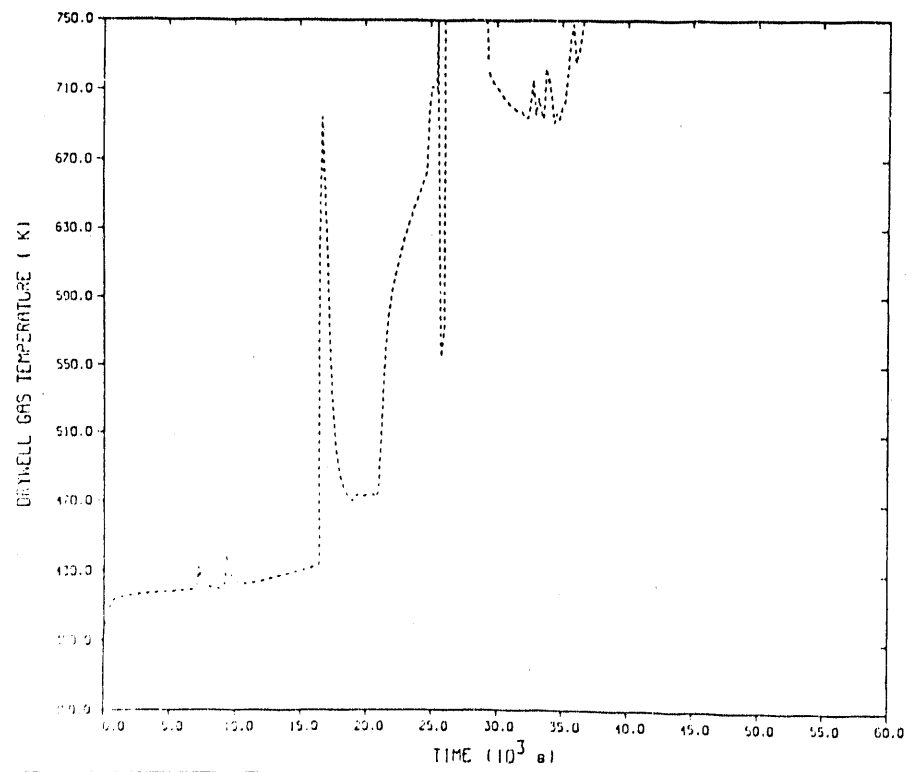


Figure 13 Temperature of Atmosphere in Drywell

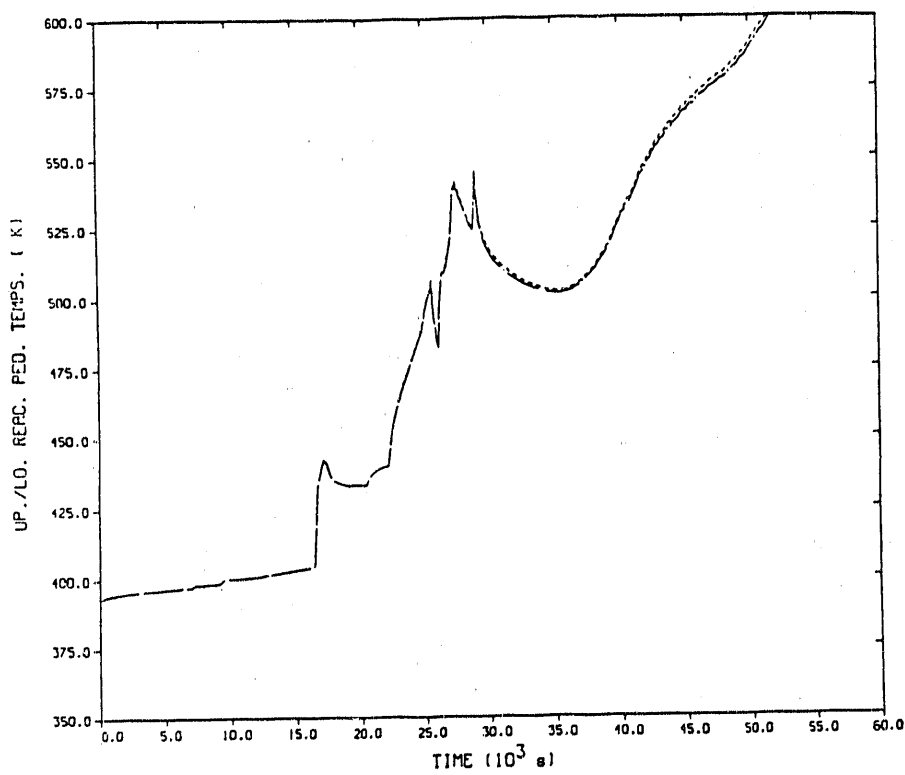


Figure 14 Temperature Response of the Upper and Lower Reactor Pedestal

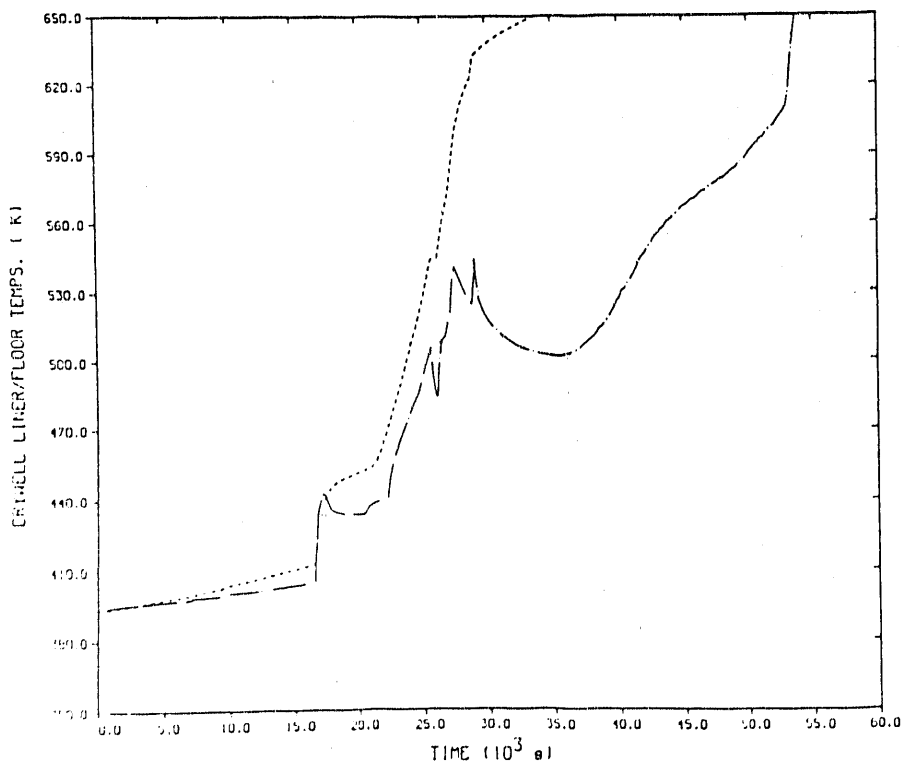


Figure 15 Temperature Response of the Drywell Liner and Floor

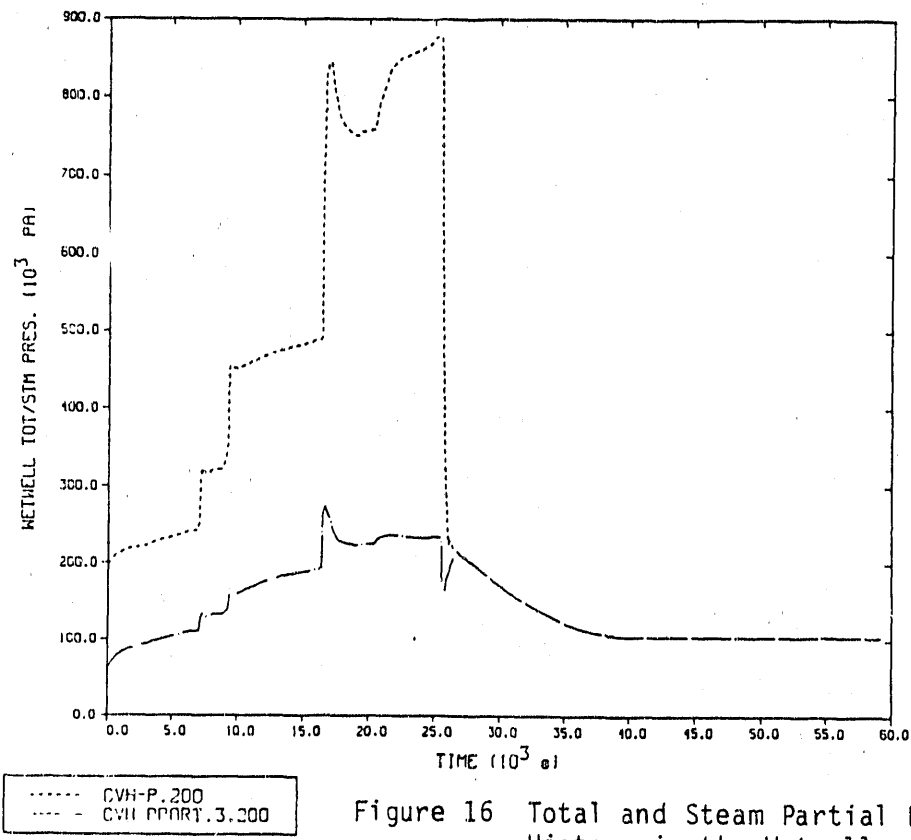


Figure 16 Total and Steam Partial Pressure History in the Wetwell

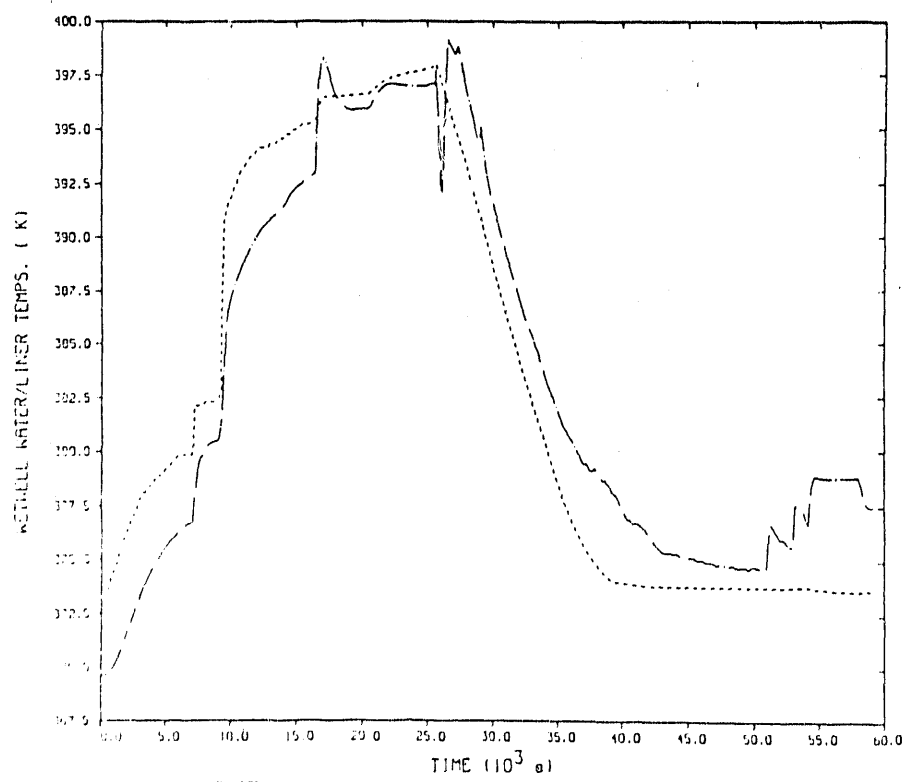


Figure 17 Temperature Response of the Wetwell Pool and Liner

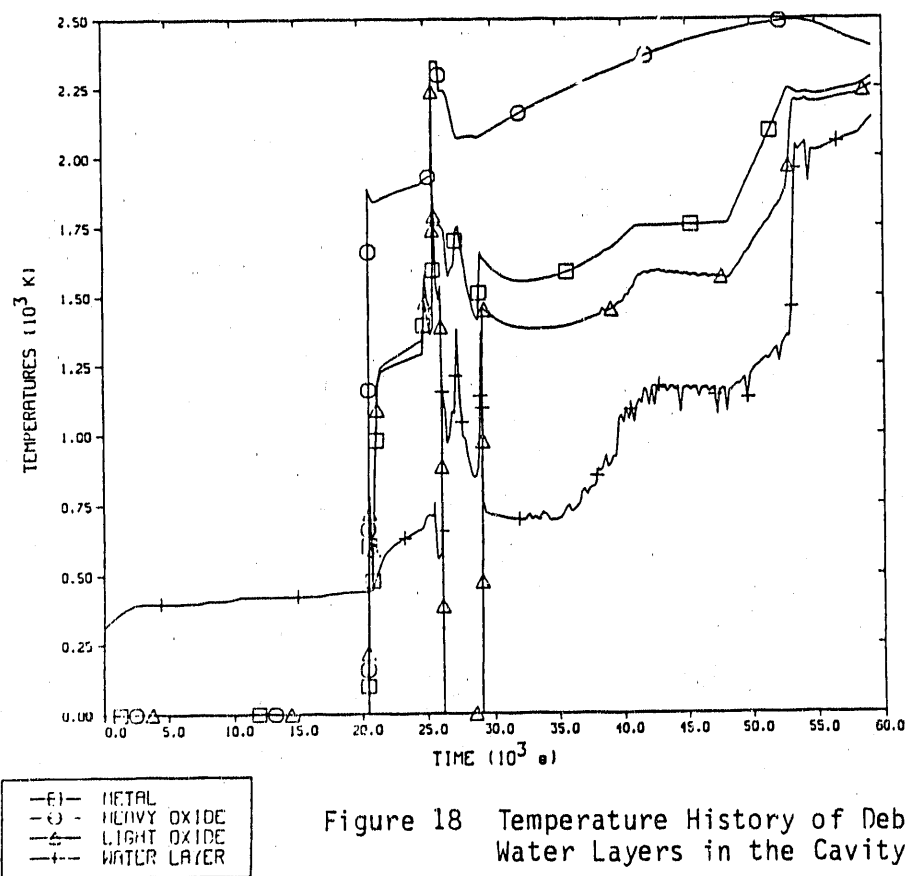


Figure 18 Temperature History of Debris and Water Layers in the Cavity

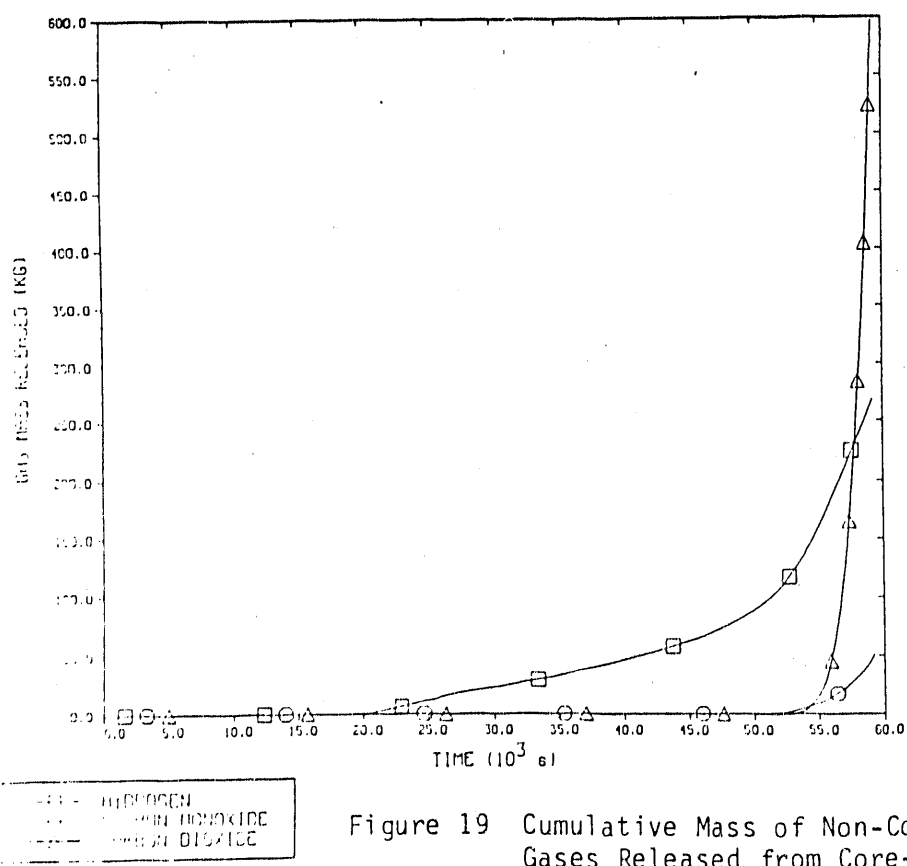


Figure 19 Cumulative Mass of Non-Condensable Gases Released from Core-Concrete Interaction

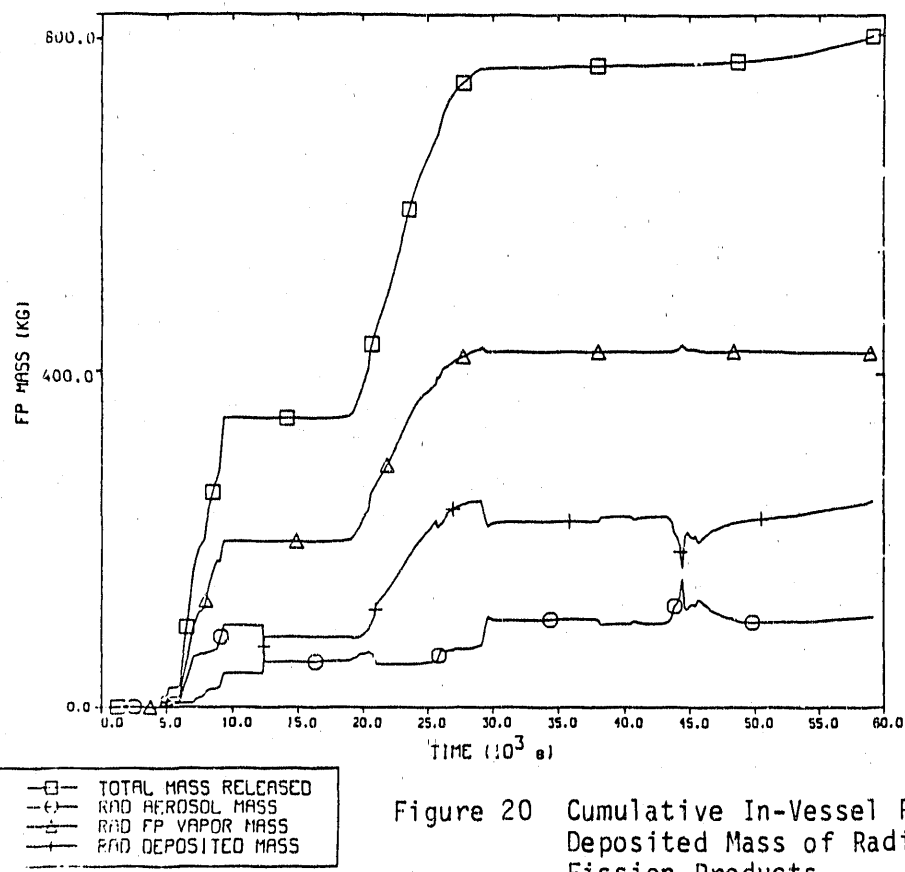


Figure 20 Cumulative In-Vessel Released and Deposited Mass of Radioactive Fission Products

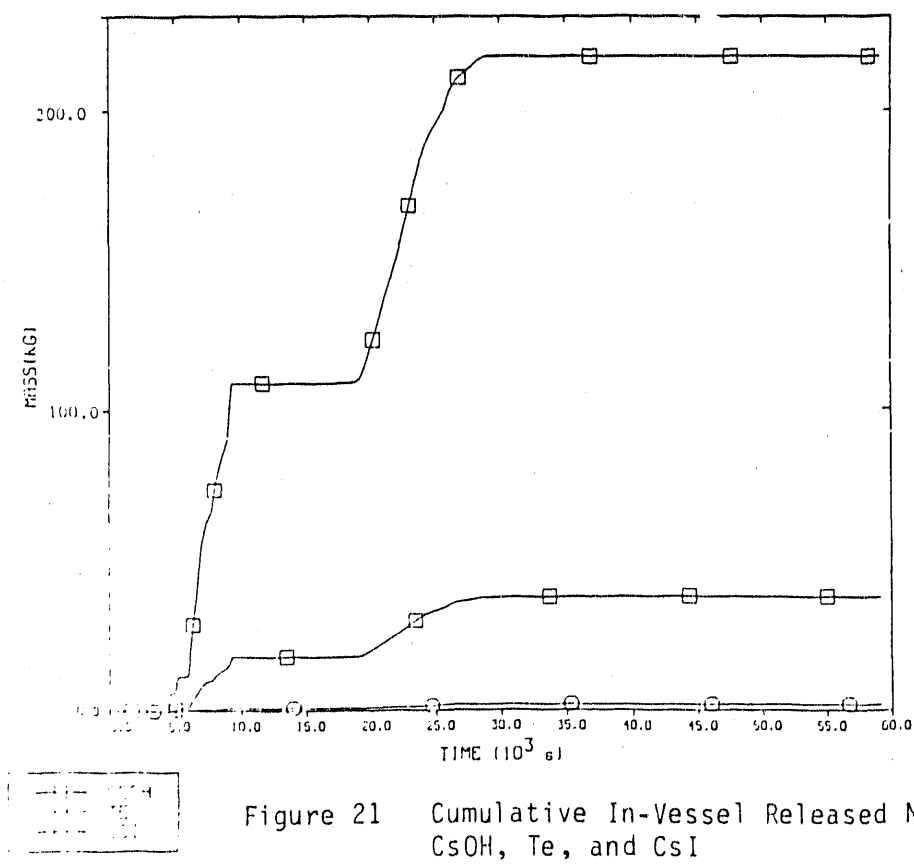


Figure 21 Cumulative In-Vessel Released Mass of CsOH, Te, and CsI

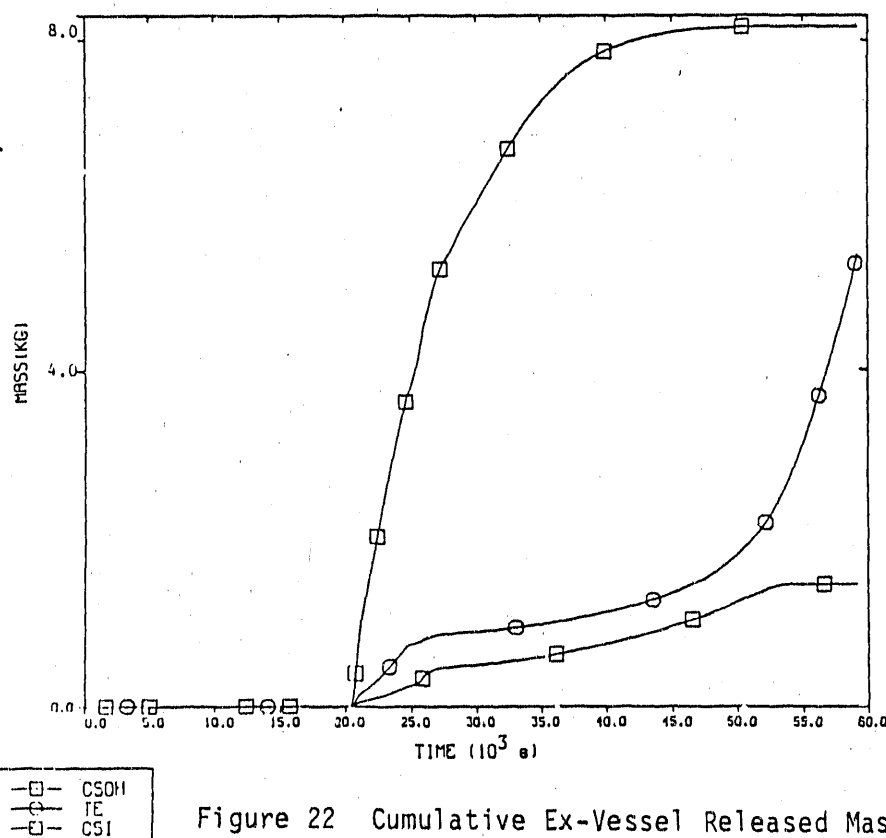


Figure 22 Cumulative Ex-Vessel Released Mass of CsOH, Te, and CsI

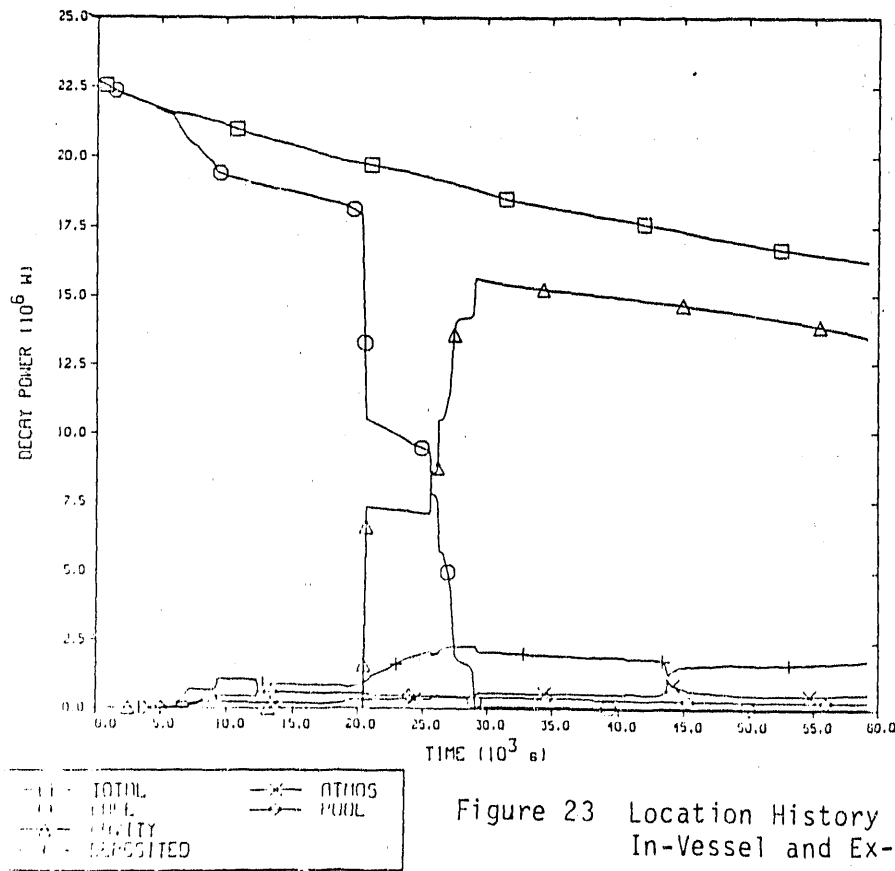


Figure 23 Location History of Decay Heat In-Vessel and Ex-Vessel

END

DATE FILMED

02/08/91

